

SYSTEM SIZE DEPENDENCE OF FINITE-SIZE EFFECTS IN ADSORBED CONFORMATIONAL PHASES OF GRAFTED POLYMERS

PAULO H.L. MARTINS^{a,†}, MICHAEL BACHMANN^{a,b,c,‡}

^aInstituto de Física, Universidade Federal de Mato Grosso
78060-900 Cuiabá (MT), Brazil

^bSoft Matter Systems Research Group, Center for Simulation Physics
The University of Georgia, Athens, GA 30602, USA

^cDepartamento de Física, Universidade Federal de Minas Gerais
31270-901 Belo Horizonte (MG), Brazil

(Received May 12, 2015)

By means of contact-density chain growth simulations, we compare thermodynamic properties of adsorption at solid substrates for two lattice polymers with 32 and 128 monomers, which gives insight into finite-size effects governing the compact phases. In both cases, we construct the entire structural phase diagrams parametrized by temperature and solvent quality, and investigate the fluctuations of macroscopic thermodynamic quantities that enable us to distinguish structural phases and to locate transition regions.

DOI:10.5506/APhysPolB.46.1219

PACS numbers: 05.10.-a, 87.15.A-, 87.15.Cc

1. Introduction

Understanding physical processes that are associated with the adsorption of soft matter at solid substrates is an exciting and challenging topic. Even though a large number of publications has reported on the progress of experimental and computational research in this field, most of the essential questions remain unanswered to this date. The central problem is that technologically interesting and also biologically relevant systems are of finite size. Numerous studies of scaling properties of the adsorption transition were performed that led to the rather exaggerated emphasis on the estimation and over-interpretation of the importance of the crossover exponent ϕ for the number of surface contacts in relation to the system size (for

[†] pmartins@fisica.ufmt.br

[‡] bachmann@smsyslab.org, url: www.smsyslab.org

very large systems) [1]. What has been neglected is the more interesting questions of geometric properties of adsorbed polymer conformations and of the thermodynamics of structural transitions between stable phases [2]. These structural properties are particularly important for biological systems and bionanotechnological applications, because structure and function of biomacromolecules are typically tightly intertwined.

In this paper, we investigate and compare for two system sizes (polymers with 32 and 128 monomers) the behavior of thermodynamic quantities in the structural phases of adsorbed polymers. Data were obtained by employing the contact-density chain-growth method [2], which is based on the multicanonical chain-growth algorithm [3] or alternatively, the flat-histogram version [4] of the pruned-enriched Rosenbluth method (PERM) [5]. In the Rosenbluth method [6], the chain is grown on a lattice by attaching one monomer after the other at the end and the growth direction is chosen randomly from the set of available unoccupied nearest-neighbor lattice sites. This creates a biased self-avoiding random walk and the statistics of all possible walks is only correct if Rosenbluth weights are introduced that correct for the bias. These Rosenbluth weights are cleverly used in the more sophisticated PERM based methods mentioned above to improve the efficiency of chain-growth algorithms substantially.

In this study, contact-density chain growth simulations were performed for a simple lattice polymer adsorption model that allows for the decoupling of energy scales and easy access to all contact-number based quantities by simple reweighting.

2. Coarse-grained lattice polymer model of adsorption

We use the simplest-possible model for a self-interacting homopolymer in the vicinity of an attractive homogeneous substrate. The configurational space is limited to a simple-cubic grid, *i.e.*, the polymer resembles an interacting self-avoiding walk on this three-dimensional lattice. Monomer–monomer interaction is attractive and short-range in that it is restricted to non-bonded nearest neighbors on the lattice. Therefore, the key parameter for the energetic state of the polymer is the number of monomer–monomer contacts, n_m . In a similar way, the energetic contribution from the interaction with the substrate originates from the number of surface contacts of the polymer, n_s . A monomer is in contact with the substrate if it is only one lattice unit away from it. We consider here a grafted polymer, in which case one end of the polymer is covalently bound to the surface and cannot desorb.

Each interaction can be assigned an energy unit and in minimal coupling, the model can be written as [2, 7]

$$E_s(n_s, n_m) = -\varepsilon(n_s + s n_m), \quad (2.1)$$

where we have introduced the global energy scale ε (which from now on is set to unity for convenience) and the ratio of respective monomer–monomer and monomer–substrate energy scales, $s > 0$. Effectively, s controls the solvent quality, *i.e.*, larger s values favor the formation of monomer–monomer contacts (poor solvent), whereas smaller values generally lead to a stronger binding to the substrate.

Extensive contact-density chain growth simulations [2] of this model were performed for lattice polymers with $N = 32$ and $N = 128$ monomers.

3. Structural hyperphase diagrams

The advantage of simulating in contact number space, and not in energy space as in conventional Monte Carlo simulations, is that the values of the external parameters, temperature T and solvent quality s , can be adjusted *after* the simulation has been performed. This is so because the result of the simulation is the contact density $g(n_s, n_m)$, which is the absolute number of states for a given pair of contact numbers. It is convenient to consider the contact numbers as appropriate order parameters that help distinguishing the structural polymer phases.

The absolute, restricted partition function (or the unnormalized probability distribution) for given contact numbers reads

$$Z_{T,s}(n_s, n_m) = g(n_s, n_m) \exp[-E_s(n_s, n_m)/k_B T] \quad (3.1)$$

and the canonical partition sum is obtained as $Z_{T,s}^{\text{can}} = \sum_{n_s, n_m} Z_{T,s}(n_s, n_m)$. The restricted partition sum allows us also to introduce the free energy in order parameter space,

$$F_{T,s}(n_s, n_m) = -k_B T \ln Z_{T,s}(n_s, n_m) = E_s(n_s, n_m) - T S(n_s, n_m), \quad (3.2)$$

where we have used the definition of the “micro-contact” entropy [7], given by $S(n_s, n_m) = k_B \ln g(n_s, n_m)$.

For both system sizes, Fig. 1 shows the map of all free energy minima $F_{T,s}^{\text{min}}(n_s, n_m)$ in (n_s, n_m) space that were found in the intervals of the external parameters $T \in [0, 10]$ and $s \in [0, 10]$, respectively. Also shown on the maps are “paths” through temperature space for $s = 0.3$ and $s = 0.8$ fixed. The paths were created by connecting the corresponding free energy minima associated with the temperatures at the fixed s value if the temperature is increased in small steps from $T = 0$ to $T = 10$.

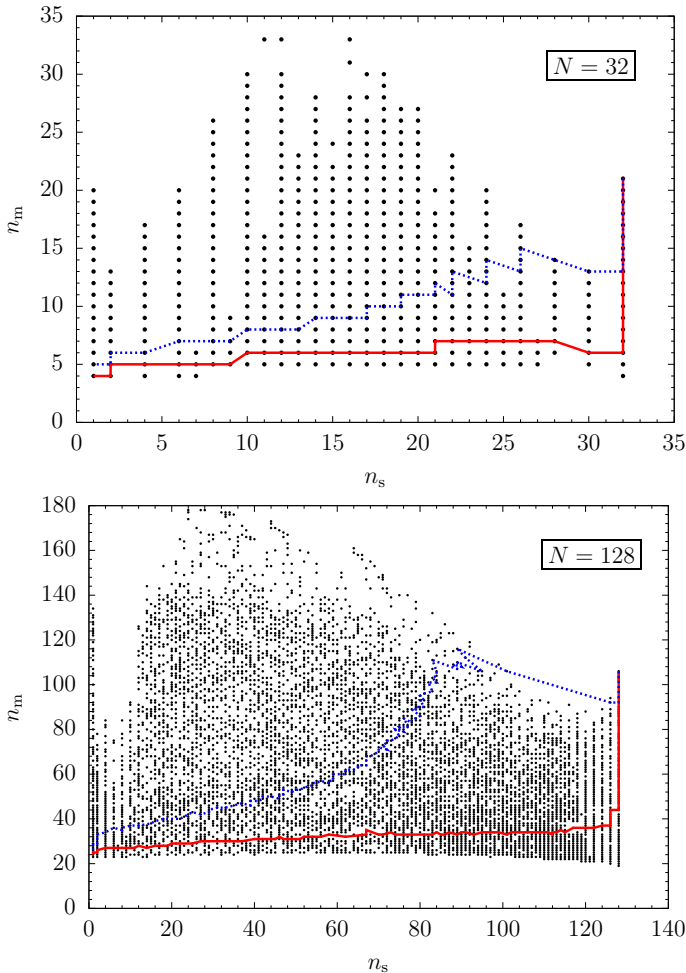


Fig. 1. Map of all free energy minima in the intervals $T \in [0, 10]$ and $s \in [0, 10]$ for the 32mer and for the 128mer. Also shown are transition paths through contact number space from $T = 0$ to $T = 10$ at $s = 0.3$ (solid line) and $s = 0.8$ (dotted), respectively.

Not surprisingly, the structure of the map for $N = 32$ (top figure) does not show many characteristic features. The “journey” (for both $s = 0.3$ and $s = 0.8$ fixed) starts at $T = 0$ with polymer conformations that possess the maximum number of surface contacts ($n_s = 32$) and the maximum number of monomer–monomer contacts in a two-dimensional configuration ($n_m = 21$). This is the film-like phase of adsorbed-compact two-dimensional polymer structures (AC1). Most interestingly, by increasing the temperature, there are different scenarios for the structural dissolution of the film, depending on

the two solvent parameter values. For $s = 0.3$, the polymer structure melts, but virtually all monomers remain in contact with the substrate, before the polymer desorbs. On the contrary, the polymer behaves differently for $s = 0.8$, in which case the polymer remains adsorbed and globular, entering a phase we call AG, and does not dissolve initially. Only gradually, the dissolution sets in upon further increase of the temperature.

The free-energy landscape of the 128mer (Fig. 1, bottom) reveals more details, in particular in the adsorption regime. The less dense regime in the top region (large n_m values) is split into peninsulas, which indicate individual compact phases with different numbers of layers [7]. The path for $s = 0.8$ exhibits a clear jump from the film-like AC1 phase into this region when passing the transition line at $T \approx 0.69$, but the resulting adsorbed macrostate is more globular (AG) than crystalline. However, the number of monomer–monomer contacts n_m increases (from 92 to a maximum value of 116) although the temperature is also increased, though this happens at the expense of losing surface contacts n_s (from 128 to 89). Further increasing of the temperature does not change n_s much, but n_m diminishes quickly; the system undergoes a second-order-like transition from globular (AG) to adsorbed expanded structures (AE), before the polymer desorbs (DE: phase of desorbed expanded structures).

The overall phase structure can be summarized by investigating the fluctuations of thermodynamic quantities. Given the fact that the contact density $g(n_s, n_m)$ is the central result of the simulation, it is possible, for instance, to calculate the specific heat landscape $c_V(T, s)$ by simple reweighting to arbitrary values of T and s

$$c_V(T, s) = \frac{1}{Nk_B T} [\langle E_s^2 \rangle(T, s) - \langle E_s \rangle^2(T, s)] , \quad (3.3)$$

where

$$\langle \dots \rangle(T, s) = \frac{1}{Z_{T,s}^{\text{can}}} \sum_{n_s, n_m} \dots g(n_s, n_m) \exp[-E_s(n_s, n_m)/k_B T] \quad (3.4)$$

is the canonical thermodynamic average in this state space. The specific heat landscape is shown as a color-coded profile for both system sizes in Fig. 2. Brighter shades correspond to larger values of c_V and indicate regions of increased thermal activity and potential transitions between structural phases. This allows us to construct the structural phase diagram. Dark lines refer to structural transitions that we think will survive in the thermodynamic limit, whereas bright lines separate phase space regions that are supposed to be governed by finite-size effects. Surprisingly, these become more apparent in the regions dominated by compact and globular structures (AC and

AG) of the 128mer, *i.e.*, for the larger system. It is, therefore, unlikely that these effects disappear in the thermodynamic limit. It is also known that this increasing complexity is not an artifact of the lattice model, as recent off-lattice simulations showed [8].

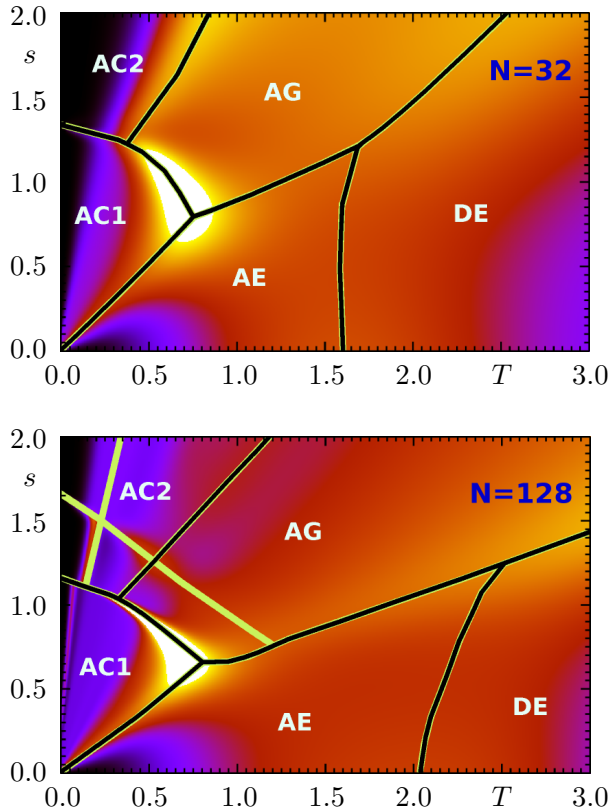


Fig. 2. Structural hyperphase diagrams of the 32mer (top) and of the 128mer (bottom) that feature the transitions between film-like, two-dimensional adsorbed conformations (AC1), adsorbed multi-layer compact (AC2), globular polymer morphologies (AG), and adsorbed expanded structures (AE). The desorption transition occurs between AE and the phase of desorbed (but still grafted) expanded (DE) conformations. The color code is associated with the specific heat; brighter areas are in correspondence with higher values of $c_V(T, s)$.

4. Thermodynamic properties of structural transitions

In Figs. 3 to 6, we have plotted various expectation values, variances, and fluctuations of quantities that are functions of the contact numbers for both system sizes. These curves are cuts through the s - T parameter space and support the interpretation of the respective specific heat landscapes in Fig. 2 as phase diagrams. The specific heat curves in section (d) of Figs. 3 to 6 are, in fact, horizontal and vertical cross sections through the specific heat landscape $c_V(T, s)$ at fixed s or T values, respectively.

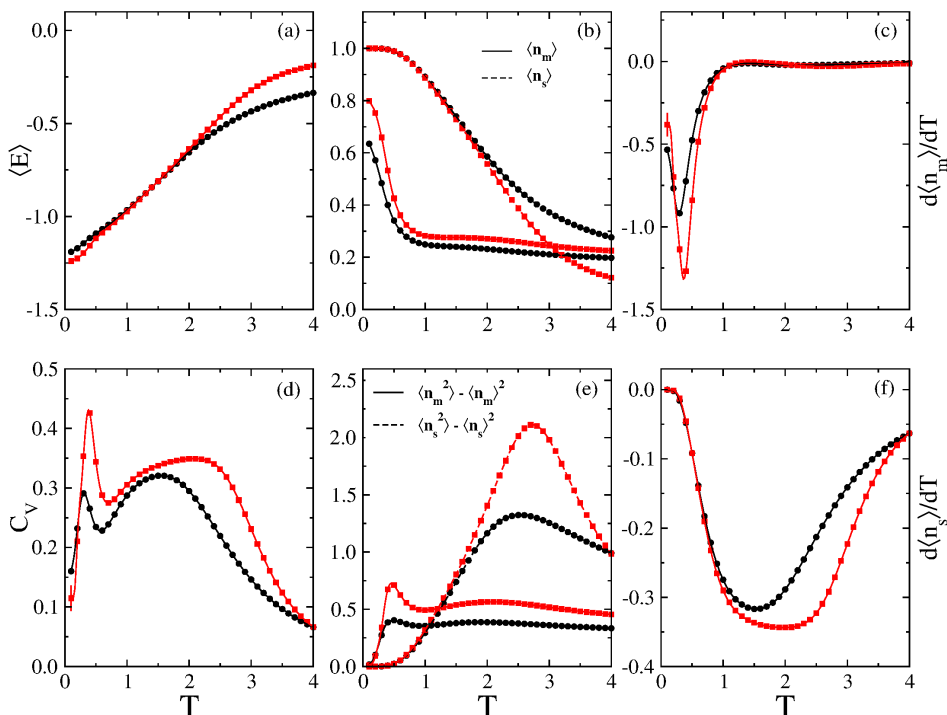


Fig. 3. Expectation values, variances, and fluctuations as functions of the temperature T for the 32mer (black curves) and for the 128mer (gray/red curves) at $s = 0.3$. Error bars were calculated using the jackknife method [2]. In most plots in this and in the subsequent figures, error bars are smaller than the symbol size.

Figure 3 summarizes the thermodynamic behavior of the system at $s = 0.3$, *i.e.*, at rather good solvent conditions. Consequently, at the low-temperature transition near $T = 0.5$, the average number of monomer–monomer contacts $\langle n_m \rangle$ drops very quickly. The number of surface contacts $\langle n_s \rangle$ remains fairly constant; the system crosses over from the structural phase of single-layer film-like conformations (AC1) to dissolved but still widely adsorbed macrostates which make up the phase of adsorbed expanded con-

formations (AE). Upon further increase of the temperature, the polymer desorbs. Now also $\langle n_s \rangle$ decreases rapidly. For the 128mer, this transition happens at a significantly higher temperature than for the 32mer ($T \approx 2.2$ vs. $T \approx 1.6$). Note that the transition temperatures as signaled by the specific heat (c) and by the fluctuations of the monomer-surface contact numbers (f) coincide pretty well, whereas the variance (e) suggests significantly higher transition points.

We re-iterate that the canonical approach to the quantitative analysis of transitions in finite systems is not optimal, because different quantities indicating thermal activity do not collapse at the same temperatures, leading to an ambiguity in the estimation of the location of transition points. This can only be cured by more modern statistical data analysis methods, such as microcanonical inflection-point analysis [2, 9], but these methods tend to be too sensitive to lattice effects as well, which is why we do not discuss these approaches any further here.

Now, for $s = 0.8$, as shown in Fig. 4, we observe near $T \approx 0.6$ a clearly anti-correlated behavior in the respective fluctuations of the two kinds of contact numbers in sections (c) and (f), as it is particularly obvious for the 128mer (gray/red curves). The conformational macrostates transform from

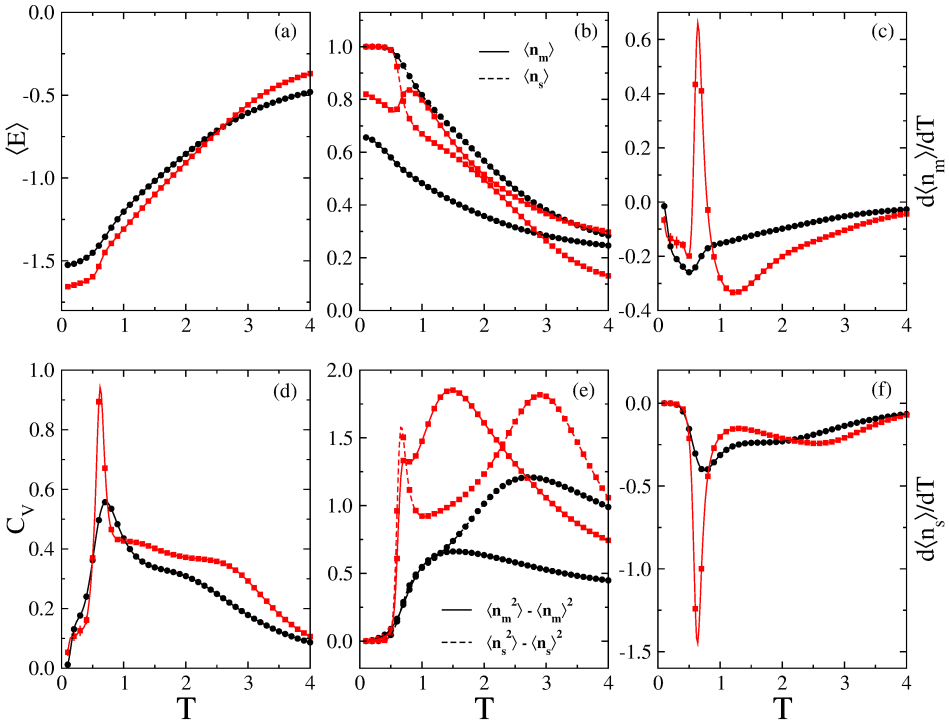


Fig. 4. The same as in Fig. 3, but with $s = 0.8$ fixed.

the single-layer AC1 phase into the phase AG of *more compact* structures (increase of $\langle n_m \rangle$), however at the expense of surface contacts. This is called a topological transition, because two-dimensional structures are replaced by three-dimensional ones. Whereas for the 32mer details of the crossover into phase AE are less obvious (the transition from AC1 to AE via AG is a rather continuous process in this case), it is way more apparent for the 128mer. The specific heat offers only a “shoulder” around $T = 1.2$ (inflection point), but the number of monomer–monomer contacts diminishes quickly in this region, which clearly indicates the dissolution of the adsorbed compact structures. It is the adsorbed-polymer equivalent of the well-known coil-globule Θ transition of free polymers. The minimum of the fluctuation (c) and the maximum of the variance (e) of $\langle n_m \rangle$ are good indicators for this process, which is still a rather weak transition (as it is for small systems in the free-polymer case as well). Eventually, the desorption transition occurs near $T = 2.5$ for the 128mer, which is best signaled by the minimum in the fluctuations of the surface contacts (f). For the 32mer, it is hardly noticeable, because many monomers have already departed from the surface in the AE phase, before the system enters the phase of desorbed expanded structures (DE).

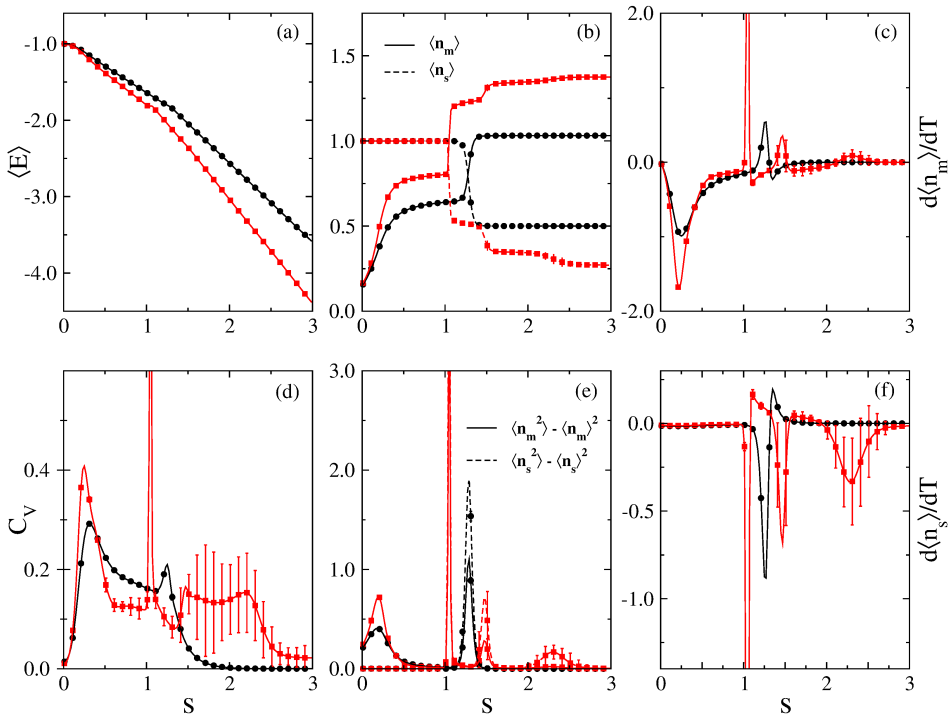


Fig. 5. The same quantities as in Fig. 3, but as functions of s at fixed temperature $T = 0.3$.

A somewhat different perspective upon the transitions in the regime of adsorbed polymers is offered if the phase space is traversed at fixed temperature by continuously varying the solvent quality parameter. For $T = 0.3$, this is shown in Fig. 5, where all routine indicators are now plotted as functions of s . The fluctuations of energy and contact numbers nicely indicate the previously described transitions between AE, AC1, and AC2. Particularly noteworthy is the increased complexity of phase AC2 for the 128mer if compared to the 32mer. Once more, in perfect anti-correlation, the contact numbers as shown in (b) signal various transitions in the compact three-dimensional phase. The resulting macrostates are multiple-layer polymer conformations. At about $s = 1.0$, the number of surface contacts drops to one half of its original value (formation of a compact double layer), reduces to about $1/3$ near $s = 1.5$ (triple-layer), and eventually to one quarter at $s \approx 2.2$ (four layers). For the 32mer, only the transition into the double-layer conformation is noticeable in the region we consider here. The number of additional monomer–monomer that can be created to overcompensate the loss of a surface contact is simply too small in this s interval.

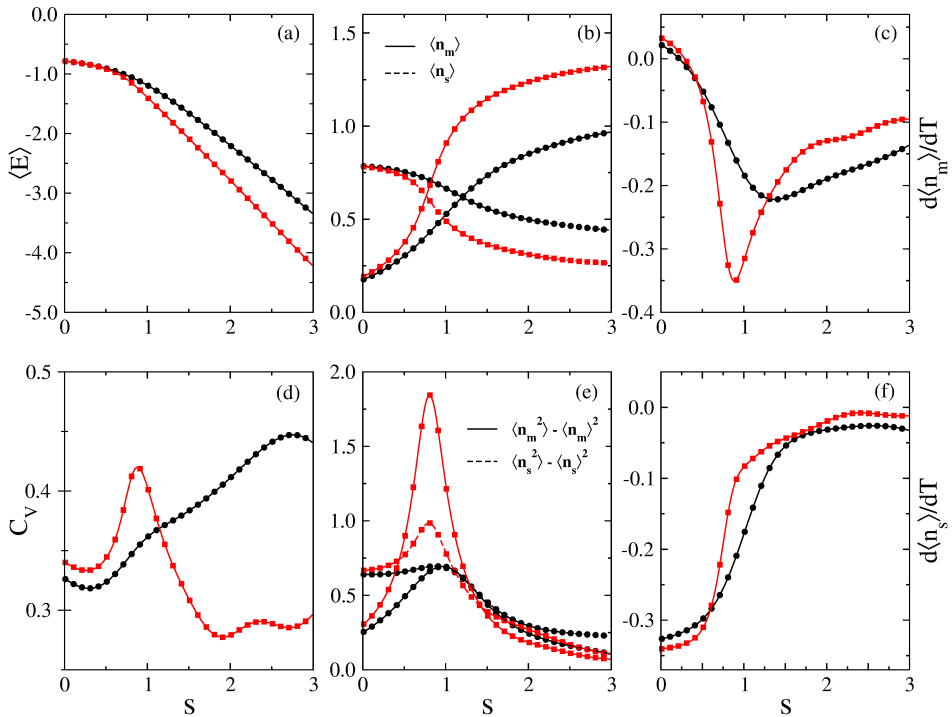


Fig. 6. The same as in Fig. 5, but at $T = 1.4$.

At the higher temperature $T = 1.4$ (Fig. 6), the $AE \Leftrightarrow AG$ transition near $s = 1$ is clearly signaled for the 128mer; for the 32mer the indication is much weaker. For higher s values, a few more signals loom up in the specific heat curve of the 128mer beyond $s = 2$, which, again, indicate the increased abundance of higher-order layered structures when AG turns over to $AC2$.

5. Summary

We have performed contact-density chain-growth computer simulations to investigate the differences in the thermodynamics of the adsorption behavior of polymers with 32 and 128 monomers grafted at a homogeneous substrate. For this purpose, we employed a simple-cubic lattice polymer model with attractive nearest-neighbor interaction between non-bonded monomers and between monomers and the substrate. The ratio of the competing energy scales, which has the physical meaning of a solvent quality parameter, was systematically varied, as was also the temperature as another external control parameter. The simplicity of the model allows us to reduce the complexity of the problem to a mere analysis of the thermodynamic behavior of the contact numbers between non-bonded monomers and between monomers and the substrate, which serve as extremely well-defined order parameters that help distinguishing the individual phases.

From various perspectives, we investigated the complete structural hyperphase diagrams. Using as the basis the minima of the free-energy landscapes in the space of the contact numbers, parametrized by the external parameters solvent quality and temperature, we obtained a first impression on the pathways of structure formation in contact number space. The thorough analysis of the profile of the specific heat landscape, as a function of solvent quality and temperature, revealed regions of phase stability, separated by structural transitions. A detailed analysis of contact-number based macroscopic thermodynamic quantities and their fluctuations supported the interpretation of the hyperphase diagram.

For both system sizes, we clearly reproduce the major structural phases (compact adsorbed phases with single and multiple layers, an adsorbed globular phase, a disordered phase of adsorbed expanded structures, and the desorbed phase). However, we also find that the complexity of the adsorbed-compact multi-layer phase of three-dimensional polymer conformations increases with the system size. In consequence, we conclude that the disappearance of subphases in this regime in the thermodynamic limit is unlikely. This sheds some new light on the understanding of the formation and stability of crystalline phases in general and in the case of adsorbed polymers, as discussed in this paper, in particular. Thorough and more detailed studies of these features remain interesting for future work.

This work has been supported partially by CNPq (Conselho Nacional de Desenvolvimento Científico e Tecnológico, Brazil) under Grant No. 402091/2012-4 and by the NSF under Grant No. DMR-1207437.

REFERENCES

- [1] For a review of ϕ estimates, see, *e.g.*, M.P. Taylor, J. Luetttmer-Strathmann, *J. Chem. Phys.* **141**, 204906 (2014).
- [2] M. Bachmann, *Thermodynamics and Statistical Mechanics of Macromolecular Systems*, Cambridge University Press, Cambridge 2014.
- [3] M. Bachmann, W. Janke, *Phys. Rev. Lett.* **91**, 208105 (2003); *J. Chem. Phys.* **120**, 6779 (2004).
- [4] T. Prellberg, J. Krawczyk, *Phys. Rev. Lett.* **92**, 120602 (2004); J. Krawczyk, A.L. Owczarek, T. Prellberg, A. Rechnitzer, *Europhys. Lett.* **70**, 726 (2005).
- [5] P. Grassberger, *Phys. Rev. E* **56**, 3682 (1997).
- [6] M.N. Rosenbluth, A.W. Rosenbluth, *J. Chem. Phys.* **23**, 356 (1955).
- [7] M. Bachmann, W. Janke, *Phys. Rev. Lett.* **95**, 058102 (2005); *Phys. Rev. E* **73**, 041802 (2006).
- [8] M. Möddel, W. Janke, M. Bachmann, *Macromolecules* **44**, 9013 (2011).
- [9] S. Schnabel, D.T. Seaton, D.P. Landau, M. Bachmann, *Phys. Rev. E* **84**, 011127 (2011).